

## Self-action of few-cycle pulses in a dispersive medium

A. A. Balakin, A. G. Litvak, V. A. Mironov, and S. A. Skobelev\*  
*Institute of Applied Physics, Russian Academy of Sciences, Nizhny Novgorod, Russia*  
 (Received 27 March 2009; published 3 December 2009)

Basing on the nonlinear wave equation as the reflection-free approximation, we study the self-focusing dynamics of laser pulses under rather general assumptions about media dispersion. The methods for qualitative investigation of the self-action dynamics of ultrashort pulses are developed. It is shown that a new effect here is steepening of the longitudinal pulse profile, which is determined by the dependence of group velocity on the amplitude. Results of numerical simulation in media without dispersion and with anomalous dispersion confirm the conclusion about outrunning formation of a shock wave during pulse self-focusing. The formation of a power spectrum of the field, which is characteristic for a shock wave, is retained also when medium ionization is taken into account. In the case of a normal-dispersion medium, nonlinear dispersion leads to a violation of the symmetry in the longitudinal splitting of the pulse in the process of self-focusing. The possibility of tuning of the optical-pulse frequency into the short-wave area is shown for the pulse self-action near the zero-dispersion point.

DOI: [10.1103/PhysRevA.80.063807](https://doi.org/10.1103/PhysRevA.80.063807)

PACS number(s): 42.65.Jx, 42.65.Sf, 42.65.Re

### I. INTRODUCTION

Femtosecond laser pulses provide unique opportunities for studying extreme light interaction with matter. Development of femtosecond technology results in creation of tools for further shortening of laser pulses and their conversion into radiation with a frequency bandwidth comparable with the carrier frequency. Theoretical study of the self-action of ultrashort laser pulses with such a broad frequency spectrum requires a modified approach that is not based on the approximation of a slowly varying envelope of the wave field. An approach to studying the dynamics of ultrashort pulses, which is widely used now, is based on supplementing the nonlinear Schrödinger equation (NSE) with the terms allowing for the dependence of group velocity on the amplitude of the wave packet (nonlinear dispersion) and for higher-order dispersion (compared with the square one) [1–7]. A great number of parameters which characterize a system hinder studying analytically the peculiarities of the self-action dynamics of ultrashort pulses by the methods of nonlinear-wave theory. One manages to achieve the required level of understanding the hierarchy of physical processes only in one-dimensional (optical fiber) systems [8]. The dominant method in the studies of self-action dynamics of three-dimensional (3D) fields is numerical simulation. This makes it possible to interpret specific experimental results for interaction of laser pulses with matter in more detail. At the same time, attempts for studying the problem analytically are rather attractive, since they allow making some general conclusions about the system dynamics.

This paper contains the analytical and numerical study of 3D ultrashort laser pulses self-action in nonlinear media. In contrast with earlier work [9], here we will focus on studying not only structural peculiarities of the field dynamics, but also the evolution of the pulse spectrum in the self-action process. In some cases, this characteristic allows making

more specific conclusions about spatiotemporal evolution of the wave field. Moreover, it is observable in experiments. In Sec. II, we derive the equation describing the evolution of a pulse with a small number of field periods. In Sec. III, the dynamics of self-action of three-dimensional wave packets is studied qualitatively. Further, we consider evolution of the field in a dispersion-free media (Sec. IV) and the influence of frequency dispersion in the media in the process of the self-action of electromagnetic waves (specifically, cases of anomalous and normal dispersion are considered in subsections A and B, respectively). In subsection C, the results of studying field self-focusing near the point of zero dispersion of group velocity are described, whereas Sec. VI presents the results of studying the dynamics of self-action of three-dimensional wave packets with account of the influence of nonlinearity saturation and medium ionization on the pulse self-focusing. In the final section, main conclusions are formulated.

### II. BASIC EQUATIONS

Let us represent the wave equation which describes propagation of a packet of electromagnetic waves along the  $z$  axis in the form

$$\frac{\partial^2 \mathbf{E}}{\partial z^2} + \Delta_{\perp} \mathbf{E} - \frac{1}{c^2} \frac{\partial^2 \mathbf{E}}{\partial t^2} = \frac{4\pi}{c^2} \frac{\partial^2 \mathbf{P}}{\partial t^2}, \quad (1)$$

where  $\Delta_{\perp} = \partial^2 / \partial x^2 + \partial^2 / \partial y^2$ , and vector  $\mathbf{P}$  is the polarization response of the medium in the field of intense radiation.

To determine the dependence  $\mathbf{P}(\mathbf{E})$ , we will use the Lorentz dispersion theory generalization for the case of strong field. Let us consider a medium consisting of a set of two oscillators with a strong different eigenfrequencies. Assuming  $\mathbf{P} = \mathbf{P}_1 + \mathbf{P}_2$  we will get a satisfactory description of a dielectric permittivity of different weakly absorbing media in the sufficiently broad frequency range [8]. Following [8] let us find the medium polarization response to the circularly polarized electric field  $\mathbf{E} = (\mathbf{x}_0 + i\mathbf{y}_0)E$ ,

\*sksa@ufp.appl.sci-nnov.ru

$$\frac{\partial^2 P_1}{\partial t^2} + \omega_o^2 P_1 + \delta |P_1|^2 P_1 = \chi \omega_o^2 E, \quad (2a)$$

$$\frac{\partial^2 P_2}{\partial t^2} = \frac{\omega_p^2}{4\pi} E. \quad (2b)$$

Here,  $\omega_o$  is the oscillator frequency,  $\delta$  is the nonlinearity parameter, and  $\chi$  is the static linear susceptibility of the medium. The second oscillator provides “plasma” dispersion (2b), and its eigenfrequency is equal to zero.

For the field with the central frequency  $\omega$  and bandwidth  $\Delta\omega$ , which is much less than the eigenfrequency  $\omega_o$ ,

$$\Delta\omega < \omega \ll \omega_o, \quad (3)$$

one can use the method of successive approximations with respect to the nonlinear parameter  $\delta$  and the nonlinearity to obtain the following formula [9] for the polarization response of the medium,

$$P_1 = \chi E - \frac{\chi}{\omega_o^2} \frac{\partial^2 E}{\partial t^2} - \frac{\delta \chi^3}{\omega_o^2} |E|^2 E. \quad (4)$$

By substituting Eqs. (2b) and (4) into Eq. (1) and passing over to the accompanying system of coordinates ( $z \rightarrow z, \tau = t - z\sqrt{\varepsilon_o}/c$ ), one can represent vectorial wave Eq. (1) for the electric field of the wave in the case of a medium with inertia-free Kerr nonlinearity as follows

$$\begin{aligned} \frac{\partial^2 E}{\partial z^2} + \Delta_{\perp} E - \frac{2\sqrt{\varepsilon_o}}{c} \frac{\partial^2 E}{\partial z \partial \tau} - \frac{\omega_p^2}{c^2} E + \frac{4\pi\chi}{c^2 \omega_o^2} \frac{\partial^4 E}{\partial \tau^4} \\ + \frac{4\pi\delta\chi^3}{c^2 \omega_o^2} \frac{\partial^2}{\partial \tau^2} (|E|^2 E) = 0, \end{aligned} \quad (5)$$

where  $\varepsilon_o = 1 + 4\pi\chi$  is the static dielectric permittivity of the medium.

It is convenient to use the evolutionary equation for wave field in the simplest form of the reduced wave equation [10–12] to perform detailed analysis of the dynamic problem. In this equation, the spatiotemporal structure of the wave field is supposed to be varying smoothly during unidirectional propagation in the media. I.e., the reflection effects [specifically, the first term in Eq. (1)] are neglected. Analysis shows that refraction is small even when the nonlinear dielectric permittivity is of order of the unity [13]. For the case of quasimonochromatic pulses, this approach corresponds to passing over to the envelope equation. We use the approximation of unidirectional propagation of the wave field along the  $z$  axis in a medium with a focusing nonlinearity ( $\chi\delta < 0$ ) to write Eq. (5) in the following form:

$$\frac{\partial}{\partial \tau} \left( \frac{\partial u}{\partial z} + \frac{\partial}{\partial \tau} (|u|^2 u) - b \frac{\partial^3 u}{\partial \tau^3} \right) = \Delta_{\perp} u - au. \quad (6)$$

Here, the following dimensionless variables are introduced:

$$z \rightarrow z \frac{2\sqrt{\varepsilon_o}\omega}{\omega_p^2}, \quad r_{\perp} \rightarrow r_{\perp} \frac{c}{\omega_p}, \quad b = \frac{4\pi\chi\omega^4}{\omega_o^2\omega_p^2},$$

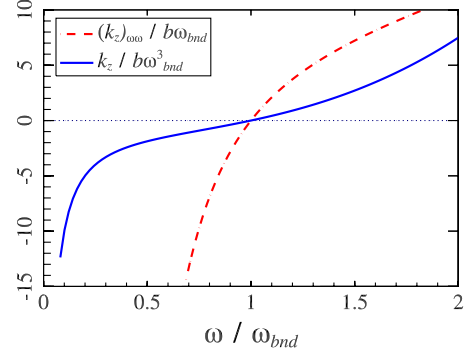


FIG. 1. (Color online) Dispersion law  $k_z(\omega)$  (solid blue line) and  $\partial^2 k_z / \partial \omega^2$  (dashed red line).

$$\tau \rightarrow \frac{\tau}{\omega}, \quad E = u \sqrt{\frac{\omega_o^2 \omega_p^2}{4\pi\delta\chi^3 \omega^2}}. \quad (7)$$

Parameters  $a$  and  $b$  determine the low-frequency and high-frequency dispersion of the medium, respectively.

It should be noted that the form of the linear part of the dielectric permittivity  $\varepsilon(\omega)$ ,

$$\varepsilon(\omega) = \varepsilon_o - \frac{a}{\omega^2} + b\omega^2 \quad (8)$$

is universal, since it contains the required number of terms to describe dispersion in a wide frequency range in the transparent area within main approximation (8). This law [Eq. (8)] can be obtained also from more general relationships of the medium dispersion theory, e.g., by using the Kramers-Kronig relationship (see, e.g., Appendix A [12,14]).

Like in the NSE case, scaling invariance of Eq. (6) makes it possible to describe the features of the system dynamics by using only two dispersion parameters, namely,  $a > 0$ , which determines the low-frequency dispersion, and  $b > 0$ , the high-frequency one. By choosing the parameters ( $a > 0, b > 0$ ), one can achieve good agreement with the experimental data, for example, for quartz glass such agreement is realized when the frequency changes by an order of magnitude [10].

In the case under consideration, the linear dispersion law for the wave  $u \sim \exp(i\omega\tau - ik_z z)$ , which propagates along  $z$  ( $\Delta_{\perp} = 0$ ), has the form

$$k_z = -a/\omega + b\omega^3. \quad (9)$$

It is possible to control the role of dispersion by changing the central frequency  $\omega$  of the wideband wave packet (see Fig. 1). Specifically, for the wave packet with the frequency  $\omega_{bnd} = (a/3b)^{1/4}$ , the parameter of group velocity dispersion (GVD)  $\alpha = \partial^2 k_z / \partial \omega^2 = 0$ . Correspondingly, for the wave fields with the frequency  $\omega \gg \omega_{bnd}$ , the field spectrum is centered in the region with normal dispersion of group velocity,  $\alpha > 0$ , and for  $\omega \ll \omega_{bnd}$ , the dispersion is anomalous ( $\alpha < 0$ ).

Note that the equation similar to Eq. (6) was used in the absence of transverse effects ( $\Delta_{\perp} \equiv 0$ ) to study the self-action of wideband pulse in a medium with the electron type of nonlinearity [12,15].

### III. QUALITATIVE STUDY OF SELF-ACTION DYNAMICS

Let us discuss separately those effects, which are not taken into account when we pass over to standard NSE. For the case of a quasimonochromatic wave packet having the form  $u = \psi(z, \mathbf{r}_\perp, \tau) e^{i\varpi\tau}$ , from Eq. (6), one can obtain the following generalized nonlinear Schrödinger equation (GNSE) for the envelope,

$$i \frac{\partial \psi}{\partial z} + \Delta_\perp \psi + \alpha(\varpi) \frac{\partial^2 \psi}{\partial \tau^2} + |\psi|^2 \psi + i\mu |\psi|^2 \frac{\partial \psi}{\partial \tau} + \sum_{n=3}^{\infty} \alpha_n \frac{\partial^n \psi}{\partial \tau^n} = 0. \quad (10)$$

To do this, one should neglect the term  $\sim 1/\varpi \partial^2 \psi / \partial z \partial \tau$  and pass over to the system of coordinates moving with the group velocity determined by the dispersion (9). Here, the parameters of higher-order dispersion  $\alpha_n = \frac{i^n \partial^n k_z}{n! \partial \omega^n}$  are determined by the coefficients of Taylor expansion of the dispersion relation (9) in the small vicinity of the carrier frequency and  $\mu = \Delta\omega / \varpi \ll 1$ .

It should be noted that the nonlinear term in Eq. (6) disintegrates into two terms in Eq. (10). The first term describes the conventional cubic nonlinearity in GNSE, and the second one, the dependence of the group velocity of the wave packet on the field amplitude (nonlinear dispersion). The latter is usually neglected in the standard NSE, since it is smaller. However, these two terms describe different effects, namely, the cubic nonlinearity results in self-focusing of the pulse, whereas the nonlinear dispersion leads to steepening of the longitudinal profile of the pulse.

To study qualitatively features of the self-action of the wave field, which are described by Eq. (6), we will use the methods similar to those used in GNSE analysis [Eq. (10)]. Localized solutions of Eq. (6) retain the total energy of the packet (“quantum number”)

$$I = \int \int_{-\infty}^{+\infty} |\phi_\pi|^2 d\tau d\mathbf{r}_\perp \quad (11)$$

and the Hamiltonian

$$H = \int \int_{-\infty}^{+\infty} \left[ |\nabla_\perp \phi|^2 - b |\phi_{\tau\pi}|^2 - \frac{1}{2} |\phi_\pi|^4 + a |\phi|^2 \right] d\tau d\mathbf{r}_\perp, \quad (12)$$

where  $u = \phi_\tau$ . Due to the “Hamiltonian nature” of Eq. (6), one can obtain the relation

$$I \cdot \frac{d^2 \langle \rho_\perp^2 \rangle}{dz^2} = 8H + 8 \int \int_{-\infty}^{+\infty} (b |\phi_{\tau\pi}|^2 - a |\phi|^2) d\tau d\mathbf{r}_\perp, \quad (13)$$

which describes the change of the efficient transverse size of the wave field

$$I \cdot \langle \rho_\perp^2 \rangle = \int \int_{-\infty}^{+\infty} \mathbf{r}_\perp^2 |\phi_\pi|^2 d\tau d\mathbf{r}_\perp. \quad (14)$$

It is seen that for the dispersion-free medium ( $a=b=0$ ), the right-hand part of Eq. (13) is proportional to the Hamiltonian of system (12) and, therefore, the distributions of the wave

field with the negative Hamiltonian  $H < 0$  collapse in the transversal direction along the finite propagation path. This conclusion stays valid for the wave packets, whose spectrum lies predominantly in the region of anomalous dispersion of group velocity ( $b \rightarrow 0$ ). In other cases, Eq. (13) shows the possibility of initial narrowing of the transverse field distribution. In Sec. V C, we will analyze Eq. (13) near the point of zero dispersion of group velocity ( $\varpi \sim \omega_{bnd}$ ) in more detail.

In what follows, we will consider the case of wave packets with a small number of field periods and convert the variables in Eq. (6). Represent  $u(z, \mathbf{r}_\perp, \tau)$  as

$$u = Y(\zeta, \boldsymbol{\eta}, \theta) / \rho(z), \quad (15)$$

where new variables are

$$\zeta = \int \frac{dz}{\rho^2(z)}, \quad \boldsymbol{\eta} = \frac{\mathbf{r}_\perp}{\rho(z)}, \quad \theta = \tau - \frac{\rho_z}{4\rho} r_\perp^2,$$

and the function  $\rho(z)$  describes the change in the transverse size of the field and transposes the point of the nonlinear focus  $z=z_0$  to infinity. This representation of the solution of Eq. (6) allows simultaneously for two processes in the system: self-focusing of the pulse and formation of the characteristic “horseshoe” structure of the field distribution, which is determined by the variable  $\theta$ .

Having transformed Eq. (15), we obtain the equation

$$\begin{aligned} \frac{\partial}{\partial \theta} \left( \frac{\partial Y}{\partial \zeta} + \frac{\partial}{\partial \theta} (|Y|^2 Y) - \frac{\rho_{zz} \rho^3}{4} \eta^2 \frac{\partial Y}{\partial \theta} \right) + \rho^2(z) \left( a Y - b \frac{\partial^4 Y}{\partial \theta^4} \right) \\ = \Delta_\perp Y. \end{aligned} \quad (16)$$

The passing over to a “collapsing” system of coordinates allows “segregating” the self-focusing process in the system and reducing the problem to studying the quasi-one-dimensional longitudinal evolution of the pulse. It is evident that the coefficient preceding the dispersion term decreases following the law  $\sim \rho^2$  and, therefore, the influence of linear dispersion becomes weaker as the pulse approaches the focal point ( $\rho(z) \rightarrow 0$ ). The typical transverse scale of the quasi-waveguide structure in new variables is of the order of unity. Thus, the key process during pulse self-focusing, becomes steepening of its longitudinal profile. Such is at least the case of the dispersion-free medium ( $a=b=0$ ), as well as the case of a medium with anomalous group velocity dispersion ( $\varpi \ll \omega_{bnd}$ ). The case of normal dispersion ( $a=0, b \neq 0$ ) requires further consideration.

### IV. DISPERSION-FREE MEDIUM ( $a=b=0$ )

Consider the case of a dispersion-free medium in more detail. Let us represent the field in the paraxial region ( $\eta \approx 0$ ) as  $Y = \mathcal{E}(\zeta, \theta) (1 - \eta^2/2)$ . Substituting this formula into Eq. (16) and setting the coefficients in front of  $\eta^0$  and  $\eta^2$  to zero, we find that for  $|\mathcal{E}|^2$  and  $\rho$ ,

$$\frac{\partial |\mathcal{E}|^2}{\partial \zeta} + 3 |\mathcal{E}|^2 \frac{\partial |\mathcal{E}|^2}{\partial \theta} \approx 0, \quad (17a)$$

$$\frac{d^2\rho}{dz^2} \approx -2 \frac{|\mathcal{E}|^2}{\rho^3}. \quad (17b)$$

When obtaining Eqs. (17), we omitted the term with the transverse Laplacian ( $\Delta_{\perp} Y \equiv 0$ ), which determines the self-focusing threshold, as well as  $|\mathcal{E}|^2$  averaged over the pulse duration  $\tau_0$  ( $|\overline{\mathcal{E}}|^2 = \int |\mathcal{E}|^2 d\theta / \tau_0$ ), since the characteristic field scale  $\rho(z)$  depends, by assumption, on  $z$  only. Formula (17b) is valid when the threshold for the wave packet self-focusing has been exceeded significantly.

Let us relate the collapse length  $z_0$  ( $\rho(z_0)=0$ ) with the length  $z_B$  of the gradient catastrophe. The value of  $z_0$  can be estimated from the equation for the efficient transverse size of the pulse [Eq. (13)]. Under the considered conditions (dispersion-free medium), Eqs. (13) and (17b) yield the same law for the variation in the pulse width in the self-focusing process [ $\rho(z) \approx \sqrt{\langle \rho_{\perp}^2(z) \rangle}$ ]. Specifically, near  $z_0$  ( $z \sim z_0$ ), we find that for the collimated wave field [ $\rho_z(z=0)=0$ ] we have

$$\rho(z) \approx \sqrt{2}\rho_0 \sqrt{1 - z/z_0}, \quad (18)$$

where  $\rho_0$  is the initial pulse width. The coordinate  $z_0$  of the focus point can be also determined by means of the integrals of the problem

$$z_0 = \frac{\rho_0}{2} \sqrt{I/|H|}. \quad (19)$$

Converting Eq. (18) for the new evolution variable, we find

$$\sqrt{\langle \rho_{\perp}^2(\xi) \rangle} \approx \sqrt{2}\rho_0 \exp(-\rho_0^2 \xi / z_0). \quad (20)$$

Note that the coefficient in front of the terms in Eq. (16), which determines the dispersion, decreases exponentially. This justifies our earlier assumptions about the neglect of the medium dispersion.

Solutions of Eq. (17a) are studied in hydrodynamics [16]. The following conclusions can be made as applied to the considered wave field. Nonuniformity of the rate, at which the points of the longitudinal profile move, leads to steepening of the back front of the pulse and formation of a shock wave in the process of its “wave-breaking” along  $\zeta_B$ . For the pulses with the duration  $\tau_0$ , from Eq. (17a) one can easily estimate the wave-breaking length

$$\zeta_B \approx \frac{\tau_0}{3|\mathcal{E}_{max}|^2}, \quad (21)$$

where  $|\mathcal{E}|_{max}$  is the maximum value of the field at the entrance to the medium ( $z=0$ ). This corresponds to the distance in terms of “old” variables

$$z_B = z_0 \left[ 1 - \exp\left(-\frac{2}{3} \frac{\rho_0^2 \tau_0}{z_0 |\mathcal{E}_{max}|^2}\right) \right], \quad (22)$$

which is slightly shorter than the self-focusing length  $z_0$ . When obtaining Eq. (22), we used the relation between  $z$  and  $\zeta$  in Eq. (15), which has the following form:

$$\zeta = \int_0^z \frac{dz}{\rho^2(z)} = -\frac{1}{2} \frac{z_0}{\rho_0^2} \ln\left(1 - \frac{z}{z_0}\right). \quad (23)$$

Note that as  $|H|$  decreases, when the self-focusing length grows as  $z_0 \sim |I/H|^{1/2}$ , the wave-breaking region retreats exponentially from the collapse point of the transverse field distribution toward the boundary of the nonlinear medium. This result ( $z_B < z_0$ ) corresponds to the self-similar solution of Eq. (6) at  $a=b=0$ ,

$$|u| = \frac{1}{z_0 - z} \Phi\left(\tau - \frac{r^2}{4(z_0 - z)} - \frac{3\Phi^2}{z_0 - z}\right), \quad (24)$$

where  $\Phi$  is an arbitrary function. Thus, singularities of a new type are formed in media without dispersion ( $a=b=0$ ) or media with the anomalous group velocity dispersion ( $b \rightarrow 0$ ). At that, the gradient catastrophe develops near the trailing edge of the pulse at a somewhat faster rate than the collapse of the wave field ( $z_B < z_0$ ).

Formation of disruptions (shock waves) is corresponded by (unremovable) dissipation at the front and consequent damping of the wave. In the case of a weak shock wave, the intensity behind the wave-breaking point ( $\zeta > \zeta_B$ ) decreases obeying the law [16]

$$|\overline{\mathcal{E}}|^2 \approx \frac{\varrho}{\sqrt{\zeta}}. \quad (25)$$

As a result, the equation for the efficient width of the wave field [Eq. (17b)] accounting the absorption at the leading edge of the envelope shock wave acquires the form

$$\frac{d^2\rho}{dz^2} \approx -\frac{2\varrho}{\sqrt{\zeta}\rho^3}, \quad (26)$$

where  $\varrho$  is the proportionality factor in Eq. (25). Solutions of this equation are modified fraction-order Bessel functions. To describe the collapse process allowing for the loss at the leading edge of the shock wave ( $z \rightarrow z_0$ ,  $\zeta \rightarrow +\infty$ ), we find

$$\frac{1}{\rho(\zeta)} \propto \sqrt{\zeta} I_{2/3}\left(\frac{4\sqrt{2\varrho}}{3} \zeta^{3/4}\right). \quad (27)$$

Getting back to the “old” variable  $z$  in Eq. (15), we finally find that

$$\rho(z) \approx \sqrt{z_0 - z} \left( \ln \frac{1}{\sqrt{z_0 - z}} \right)^{-1/6} \Big|_{z \rightarrow z_0} \sim \sqrt{z_0 - z}. \quad (28)$$

Despite the unremovable dissipation in the system, the behavior of the pulse width [Eqs. (17b) and (28)] in the region of the nonlinear focus ( $z \sim z_0$ ) remains the same and satisfies the relation (18) [11].

To illustrate the peculiarities of the self-action for pulses with a small number of field periods (few optical cycle), let us refer to solving Eq. (6) numerically. Qualitative research showed that pulse self-focusing and front steepening occur almost simultaneously. It means that self-compression of the wave field must be accompanied by noticeable widening of the spectrum and dissipation at the leading edge of the shock wave. For the numerical simulation, Eq. (6) is supplemented

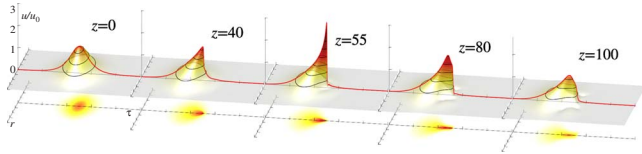


FIG. 2. (Color online) Dynamics of the circularly polarized field  $|u(z, \tau, r_{\perp})|$  in the dispersion-free medium ( $a=0$ ,  $b=0$ ) for  $\gamma=0.04$ . Distribution of the circularly polarized field over the boundary of the nonlinear medium  $u=0.6e^{i\tau}/\cosh(0.3\tau)\exp(-r_{\perp}^2/100)$ . Red line is pulse intensity  $|u(z, \tau, r_{\perp}=0)|$  at the axis. The transverse coordinate  $r$  is perpendicular to the plane of the figure.

with the diffusion-type term  $\gamma\partial^3 u/\partial\tau^3$  to stabilize the gradient catastrophe. This term is equivalent to viscosity in hydrodynamics and is usually added to equation within the theory of weak shock waves.

$$\frac{\partial}{\partial\tau}\left(\frac{\partial u}{\partial z} + \frac{\partial}{\partial\tau}(|u|^2 u) - \gamma\frac{\partial^2 u}{\partial\tau^2}\right) = \Delta_{\perp} u. \quad (29)$$

This term appears naturally when one takes into account the attenuation in the oscillator Eq. (2a). For the sake of illustration, Fig. 2 shows the results of modeling numerically the evolution of the initial distribution of the field

$$u = 0.6 \exp\left(-\frac{r_{\perp}^2}{100}\right) \frac{e^{i\tau}}{\cosh(0.3\tau)} \quad (30)$$

in a dispersion-free medium for  $\gamma=0.04$ . It is seen that the key process in the self-action dynamics for an ultrashort pulse is the steepening of the longitudinal profile and formation of a rather sharp transition zone. This is a common scenario for dispersion-free media. Numerical calculations demonstrate the presence of rather long intervals, in which the field spectrum decreases obeying the power law. Calculations [20] yield the following law for the field spectrum at the system axis ( $r_{\perp}=0$ ),

$$S(\omega) = \left| \int_{-\infty}^{+\infty} u(\tau, r_{\perp}=0) e^{i\omega\tau} d\tau \right| \sim \frac{1}{\omega}. \quad (31)$$

This law is realized in the interval from  $z=50$  to  $z=75$ , i.e., in the region with a jump in the field, which is typical for the shock wave.

To conclude this section, let us estimate the self-focusing length  $z_0$  using Eq. (13) in the dispersion-free medium ( $a=b=0$ ). For the distribution of the ‘‘potential’’ of the field in the form

$$\phi = \mathcal{A} \frac{\exp(i\omega\tau)}{\cosh(\pi\tau/\tau_p)} \exp\left(-\frac{r_{\perp}^2}{2\rho_0^2}\right), \quad (32)$$

one can evaluate the Hamiltonian using Eq. (12),

$$H = 2\pi\mathcal{A}^2\tau_p \left\{ 1 - \frac{I[35\chi^4 + 14\chi^2 + 3]}{140\pi\tau_p^3(1+3\chi^2)} \right\}, \quad (33)$$

where

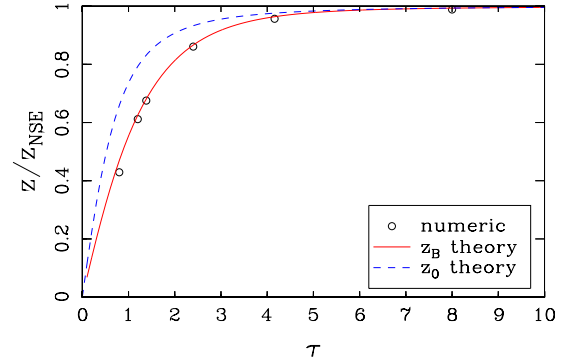


FIG. 3. (Color online) Self-focusing length  $z_0$  (blue dashed line), calculated by Eq. (34); red line is the wave-breaking length calculated by Eq. (22);  $\circ$  shows the length of singularity formation, which was obtained by solving numerically Eq. (6) for  $a=b=0$ .

$$I = \frac{2\pi\mathcal{A}^2\rho_0^2}{3\tau_p}(1+3\chi^2), \quad \chi = \omega\tau_p.$$

For the collimated wave packet ( $\rho_z(z=0)=0$ ), the coordinate of the focal point has the form

$$z_0 = \frac{\rho_0}{2} \sqrt{\frac{I}{|H|}} = \frac{\rho_0^2}{2\sqrt{3}\tau_p} \frac{\sqrt{1+3\chi^2}}{\sqrt{\frac{I}{I_{cr}} - 1}}, \quad (34)$$

where  $I_{cr}$  is the critical energy for the self-focusing of the wave packet

$$I_{cr} = \frac{140\pi\tau_p^3[1+3\chi^2]}{35\chi^4 + 14\chi^2 + 3}. \quad (35)$$

It yields, specifically, the formula for the duration of the singularity formation for a quasimonochromatic pulse ( $\chi = \omega\tau_p \gg 1$ )  $z_0^m$  [17], which is well known in the self-focusing theory,

$$z_0|_{\omega\tau_p \gg 1} = z_0^m = \frac{\rho_0^2\omega}{2} \frac{1}{\sqrt{\frac{P}{P_{cr}} - 1}}, \quad (36)$$

where  $P$  is the beam power

$$P = \int_{r_{\perp}} |\phi_{\pi}|^2 dr_{\perp} = \pi\mathcal{A}^2\omega^2\rho_0^2, \quad \text{and} \quad (37)$$

$P_{cr}$  is the critical self-focusing power.

Figure 3 shows the singularity formation length  $z_0$  as a function of the pulse duration  $\tau_p$  for the following fixed parameters of the wave field:  $\rho_0$ ,  $\mathcal{A}$ , and  $\omega$ . The value of  $z_0$  is normalized to  $z_0^m$ . As seen from Fig. 3, the length  $z_0$  decreases with the decrease in the duration of the electromagnetic pulse. For example, for the pulse duration  $\tau_p=0.5$  ( $\omega=1$ ), the length of singularity formation is  $z_0 \approx 0.5z_0^m$ .

Summing the aforesaid up, one can say basing on Eq. (34) that the distinctive feature in the self-action dynamics of ultrashort pulses in a medium with cubic nonlinearity (under the conditions of steepening of the longitudinal pulse profile) is associated with the decrease in the self-focusing length  $z_0$

in comparison with quasimonochromatic one  $z_0^m$  as the pulse duration  $\tau_p$  decreases for fixed pulse parameters:  $\rho_0$ ,  $\mathcal{A}$ , and  $\omega$ . This effect becomes most visible for extremely short pulses. The reason for this decrease is the additional longitudinal energy flow toward the singularity, which is caused by the nonuniformity of the rate, at which the points of the longitudinal profile move, as well as the transverse energy flow from the pulse periphery toward its center. As seen from Fig. 3, the results of modeling Eq. (6) numerically (circles) agree quantitatively with the qualitative study of Eq. (34) (solid blue line).

**V. DISPERSIVE MEDIUM**

Consider now peculiarities of self-focusing of wave fields in the media with the predominant anomalous ( $b \rightarrow 0$ ) and normal ( $a \rightarrow 0$ ) dispersion of the group velocity. For such cases, the self-action dynamics of quasimonochromatic wave packets is thoroughly studied in [6,8,18,19]. Here, we will discuss the features which are specific for the pulses having durations of several periods of field oscillations.

**A. Anomalous dispersion  $\varpi \ll \omega_{bnd}$**

In this case, the self-action scenario is similar to that observed for the self-focusing in a dispersion-free medium (see Fig. 2). In accordance with the qualitative scenario considered above, the process of the increase in the field amplitude is accompanied with fast steepening of the trailing edge of the wave packet. The absence of dispersion at high frequencies leads to formation of an envelope shock wave. That is why, as seen from Eq. (16), the influence of low-frequency dispersion reduces as the transverse size of the wave packet decreases.

Dispersion spreading of ultrashort pulses leads to some increase of their duration. In a medium with low-frequency (anomalous) dispersion, the spectrum decreases faster than in a dispersion-free medium ( $a=b=0$ ). Thus, in a medium with anomalous group velocity dispersion, numerical calculations for the initial distribution

$$u = 0.6 \exp\left(-\frac{r_{\perp}^2}{200}\right) \frac{\exp(i\tau)}{\cosh(0.3\tau)} \tag{38}$$

yield the following law for the field spectrum on the axis  $r = 0$  (see Fig. 4),

$$S(\omega) \sim \frac{1}{\omega^{3/2}}. \tag{39}$$

The corresponding time dependence  $u \sim \sqrt{\tau}$  is characterized by the infinite derivative at  $\tau=0$ . It means that low-frequency dispersion cannot prevent the gradient catastrophe entirely. However, it modifies the field structure in the transition area. Numerical analysis of Eq. (6) for  $a=1$  and  $b=0$  shows that the spectrum  $\omega^{-3/2}$  takes place in the interval from  $z=40$  to  $z=60$ . It should be added that in the process of absorption at the front of the shock wave, pulse energy (11) decreased by several times. As a result, the Hamiltonian of the system becomes positive and, corresponding to Eq. (13), the pulse starts spreading in the transverse direction.

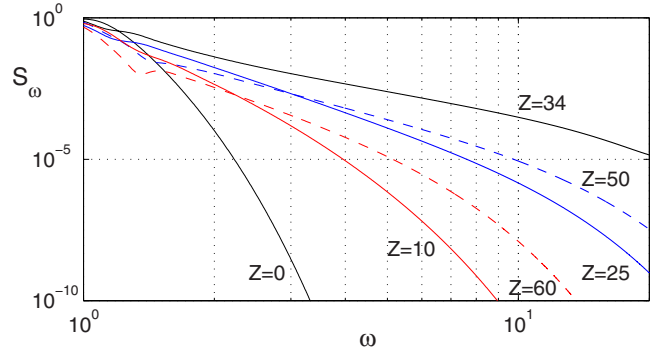


FIG. 4. (Color online) Short-wave part of the spectrum power  $S^2(\omega > 1)$  on the system axis for  $z=0, 10, 25, 34, 50,$  and  $60$  when  $a=1$  and  $b=0$  ( $\omega_{bnd} = +\infty$ ).

**B. Normal dispersion  $\varpi \gg \omega_{bnd}$**

The main regime of the self-action of quasimonochromatic wave packet in a media with normal dispersion is associated with the development of the instability of the longitudinal fragmentation of the packet [18]. The corresponding process for the case of an ultrashort pulse,

$$u = 0.8 \exp\left(-\frac{r_{\perp}^2}{200}\right) \frac{\exp(i\omega\tau)}{\cosh(0.3\tau)}, \tag{40}$$

is shown in Fig. 5. It is seen that the steepening of the trailing edge evolves simultaneously with the wave packet fragmentation [18]. As a result of splitting, a more intense pulse is formed near the trailing edge. High-frequency medium dispersion stabilizes the wave-breaking of the envelope profile, and leads further to strong spreading of the trailing edge of the pulse. As in the case of quasimonochromatic wave packets [18], one cannot prove rigorously the existence of the collapse for an ultrashort pulse. The limitation of the maximum amplitude of the quasimonochromatic field is connected with the longitudinal fragmentation of the packet. Despite the formation of sufficiently steep fronts, there are no intervals with the power-law dependence in the spectrum, as in the previous cases (without dispersion and with anomalous dispersion). This can be explained by the fact that in the paraxial region, the self-action dynamics is described by the

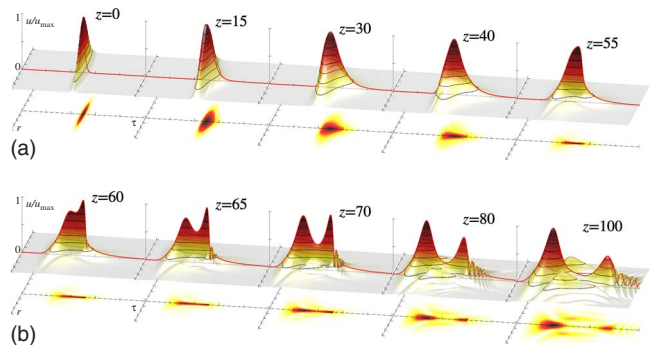


FIG. 5. (Color online) Dynamics of the circularly polarized field  $|u(z, \tau, r)|$  in a medium with the normal-dispersion law ( $a=0, b=1$ ). Distribution of the circularly polarized field at the nonlinear-medium boundary  $u=0.8e^{i\tau}/\cosh(0.3\tau)\exp(-r_{\perp}^2/200)$ .

modified Korteweg-de-Vries (KdV) equation. The possibility of longitudinal profile steepening is well known within the frame of KdV equation and is determined by high-frequency dispersion. Self-action peculiarities for such case appear due to the concurrence of envelope steepening and pulse splitting. As a result, the symmetry of pulse splitting (which is well studied in media without nonlinear dispersion) is broken and more intense pulse is formed at trailing edge.

### C. “Zero” dispersion of group velocity ( $\varpi \sim \omega_{bnd}$ )

As it has been noted above, from analysis of sufficient self-focusing condition (13), one cannot make any certain conclusions about the collapse. However, one can see that there is a class of initial field distributions, for which the relation

$$\int_{r_{\perp}} \int_{-\infty}^{+\infty} (b|\phi_{\tau\tau}|^2 - a|\phi|^2) d\tau dr_{\perp} = 0 \quad (41)$$

is fulfilled. This is the integral condition for compensation of the contributions made by the areas of normal and anomalous dispersion. For such distributions, the sufficient self-focusing condition ( $H < 0$ ) has initially the same form as those for the dispersion-free medium ( $a=b=0$ ).

For distributions of the “potential” in the form

$$\phi = \Xi \exp\left(-\frac{r_{\perp}^2}{\rho_0^2}\right) \exp\left(-\frac{\tau^2}{\tau_p^2} + i\omega\tau\right), \quad (42)$$

one can easily choose  $\omega$  and  $\tau_p$  such as to satisfy Eq. (41). As a result, for the pulse parameters ( $\omega, \tau_p$ ), we find the relation

$$\tau_p^4(\omega^4 - 3\omega_{bnd}^4) + 6\omega^2\tau_p^2 + 3 = 0. \quad (43)$$

This means that at least at the initial stage, the evolution of such specially designed distributions (42) will take place in the same way as in the dispersion-free medium.

For the sake of simplicity, let us consider the case when  $\omega_{bnd} = \omega$ . It follows from Eq. (43) that

$$\tau_p = \sqrt{\frac{3 + \sqrt{15}}{2\omega_{bnd}^2}}. \quad (44)$$

Distributions of the strength of the electric field and the frequency spectrum for this case are shown in Fig. 6. As seen from Fig. 6(a), the pulse duration at a level of 0.5 field intensity is  $\tau_{1/2} \approx 2.8$ , which is less than one field period, which amounts to  $2\pi$ . The dashed line in Fig. 6(b) shows the position of the point of zero dispersion of group velocity, which was determined by dispersion of Eq. (9). As seen from Fig. 6,  $\omega_{bnd}$  lies to the left of the spectrum maximum.

Integrals ( $H, I$ ) of the problem for distribution (42) have the form

$$\begin{aligned} H &= \frac{\pi^{3/2}\Xi^2\tau_p}{\sqrt{2}} \left\{ 1 - \frac{\sqrt{2}\Xi^2\rho_0^2}{16\tau_p^4} \left[ (\omega\tau_p)^4 + (\omega\tau_p)^2 + \frac{3}{4} \right] \right\} \\ &= \frac{\pi^{3/2}\Xi^2\tau_p}{\sqrt{2}} \left( 1 - \frac{I}{I_{cr}} \right), \end{aligned} \quad (45)$$

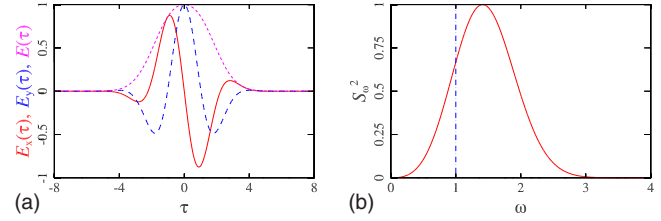


FIG. 6. (Color online) Distribution of the field (a) and spectrum (b) of the electric-field strength for  $\omega = \omega_{bnd} = 1$ . (a) Solid red line is the  $E_x(\tau)$  component, dashed blue line is  $E_y(\tau)$ , magenta dotted line is the distribution of the field envelope  $E(\tau) = \sqrt{E_x^2 + E_y^2}$ . The field period for this case is  $2\pi$ . (b) Solid red line is spectrum intensity, and dashed blue line is the position of the point of zero dispersion of group velocity.

$$I = \frac{\pi^{3/2}\Xi^2\rho_0^2}{2^{3/2}\tau_p} [(\omega\tau_p)^2 + 1], \quad (46)$$

where

$$I_{cr} = \frac{4\pi^{3/2}\tau_p^3 [(\omega\tau_p)^2 + 1]}{(\omega\tau_p)^4 + (\omega\tau_p)^2 + 3/4}. \quad (47)$$

From Eq. (45), it is seen that the initial narrowing of the transverse field distribution will take place when  $H < 0$ , i.e., when  $I > I_{cr}$ .

Now, refer to the results of numerical simulation. For the sake of illustration, Fig. 7 shows the results of numerical study of the evolution for the initial field distribution (42),

$$u = \phi_{\tau} \quad \phi = 0.26 \exp\left(-\frac{r_{\perp}^2}{550}\right) \exp\left(i\omega_{bnd}\tau - \frac{\tau^2}{\tau_p^2}\right) \quad (48)$$

in a medium with the zero-dispersion point of the group velocity  $\omega_{bnd} = 1.2$ . Here,  $\tau_p$  obeys the formula (44). From Fig. 7 it is seen that the key process is self-focusing of the field in the transverse direction. It should be noted that there was an insignificant increase [by several times, see Fig. 8(a)], in the pulse duration during the nonlinear dynamic process. Therefore, it justifies our assumption that the evolution of the specially designed field distributions should proceed as in the dispersion-free medium.

In the case under consideration, a distinctive feature is strong modification of the spectrum. As seen from Fig. 8(b), strong widening of the spectrum by about two octaves takes place. It should be added that in the process of pulse propagation [see Fig. 8(b)], the wave frequency tunes to the short-wave region in the paraxial area. This spectrum modification can be explained by the four-wave interaction

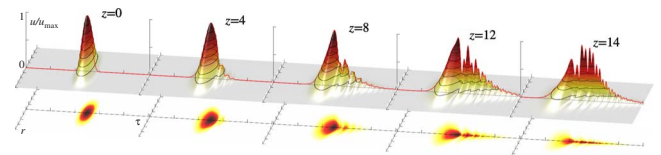


FIG. 7. (Color online) Dynamics of the circularly polarized field  $|u(z, \tau, r_{\perp})|$  in a medium with the point of zero dispersion of group velocity  $\omega_{bnd} = 1.2$ .

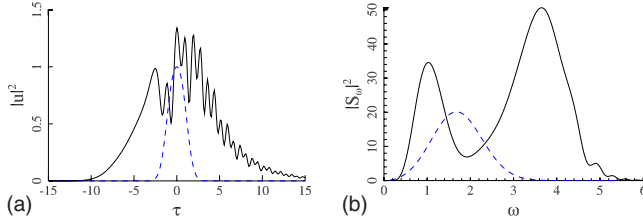


FIG. 8. (Color online) Distributions of the field intensity (a) and the spectrum intensity (b) at the entrance to the nonlinear medium (dash) and near the focal area (solid).

$$2\omega_{\star} = \omega_1 + \omega_2, \quad (49a)$$

$$2k_z(\omega_{\star}) = k_z(\omega_1) + k_z(\omega_2), \quad (49b)$$

where  $\omega_{\star}$  is the spectrum component of the incident wave. Assuming  $\omega_1 = \omega_{\star} + \Delta$  and  $\omega_2 = \omega_{\star} - \Delta$ , and using the dispersion relation in the paraxial area (9)

$$k_z(\omega) = -\frac{a}{\omega} + b\omega^3,$$

we will find the following expression for  $\Delta$ :

$$\Delta = \omega_{\star} \sqrt{1 - \left(\frac{\omega_{bnd}}{\omega_{\star}}\right)^4}. \quad (50)$$

As follows from Eq. (50), the four-wave interaction condition is fulfilled for any spectral harmonic  $\omega_{\star}$  exceeding  $\omega_{bnd}$  ( $\omega_{\star} > \omega_{bnd}$ ). As a result of this nonlinear process, the energy from the high-frequency spectrum is pumped over from the high-frequency part of the spectrum into both the high-frequency part ( $\omega > \omega_{bnd}$ ) and the low-frequency part ( $\omega < \omega_{bnd}$ ), i.e., splitting of the spectrum occurs near  $\omega \approx \omega_{bnd}$ . To study this effect, we will fix the pulse parameters but start varying the position of the point of group velocity zero-dispersion relative to the radiation carrier frequency. Figure 9 shows the results of numerical simulation of the spectrum evolution on the system axis along the evolution variable for two cases:  $\omega_{bnd} = 0.86$  and  $\omega_{bnd} = 1.02$  ( $\omega = 1$ ). As seen from Fig. 9, at the initial stage of pulse self-focusing, the spectrum splits near the point  $\omega \approx \omega_{bnd}$ . The position of  $\omega_{bnd}$  is shown by a bold red line. Then, as the radiation self-focusing proceeds, the frequency of the optical pulse is converted into the short-wave area. In this case, as shown by the numerical simulation, one can control the position of the high-

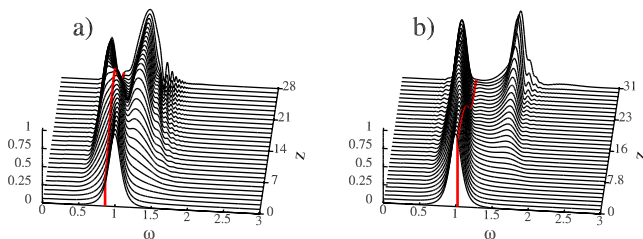


FIG. 9. (Color online) Spectrum  $S_{\omega}(\omega)$  evolution on the system axis along the evolution variable for two cases:  $\omega_{bnd} = 0.86$  (a) and  $\omega_{bnd} = 1.02$  (b). Here red line shows the position of the zero dispersion of group velocity  $\omega_{bnd}$ .

frequency satellite by changing the frequency  $\omega_{bnd}$ . As seen from Fig. 9, the amplitude of the spectral intensity in the short-wave part is comparable with that in the region  $\omega < \omega_{bnd}$  or exceeds it. This result differs from the one-dimensional case [12] and is connected with the radiation self-focusing, which leads to an additional energy flow into the paraxial area.

It is important that such a strong modification of the laser pulse spectrum leads to formation of a spatiotemporal distribution of the field in the form of corrugations (see Fig. 7). Really, since the field dynamics occurs in a medium with dispersion, it leads to situation when the “blue” spectral components are situated in the front part of the pulse (left), whereas the “red” ones, in the rear part (right). It is clear that the nonlinear interaction will result in stronger focusing of the front part of the pulse compared with the rear part of the wave packet. This is connected with the fact that the critical self-focusing power is inversely to the square of the frequency ( $P_{cr} \sim \omega^{-2}$ ).

## VI. ACCOUNT OF OTHER PROCESSES LIMITING THE WAVE-FIELD COLLAPSE

Numerical investigation of the pulse self-focusing in a dispersion-free medium and a medium with anomalous dispersion showed that the field evolution does not depend on the value of the “electromagnetic” viscosity (for its sufficiently low values), i.e., it is universal. In this case, as the field becomes stronger, its amplitude can exceed the value requiring the account of other factors. In this section, we will consider how nonlinearity saturation (VIA) and medium ionization (VIB) will affect the above conclusions about structural peculiarities of self-focusing of ultrashort pulses.

### A. Nonlinearity saturation

In numerical simulations, the nonlinearity saturation was modeled by replacing  $|u|^2$  with  $|u|^2 - \beta|u|^4$  in the second term in initial Eq. (6),

$$\frac{\partial}{\partial \tau} \left( \frac{\partial u}{\partial z} + \frac{\partial}{\partial \tau} [ |u|^2 u - \beta |u|^4 u ] \right) = \Delta_{\perp} u - au. \quad (51)$$

Calculations show that the obtained results stay valid up to  $\beta \approx 0.15$ . Figure 10 presents the data about formation of power spectrum during wave breaking of the wave field in a medium with anomalous dispersion of group velocity for various values of the saturation parameter  $\beta$ . It is seen that power spectrum is formed also at  $\beta > 0.15$ . However, in this case, the decrease law is faster. Such spectrum corresponds to formation of an infinite derivative in the field distribution in the process of steepening of the longitudinal profile. As follows from Fig. 11, nonlinearity saturation leads to the evident effect of a decrease in the maximum field amplitude and, hence, to an increase in the length of the gradient catastrophe formation. As a result, the distribution of the field becomes characteristically terraced (see Fig. 12), which differs noticeably from the structure for  $\beta = 0$ .



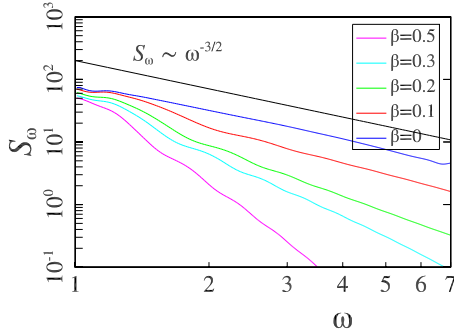


FIG. 10. (Color online) Short-wave part of the spectral power  $S^2(\omega > 1)$  on the axis in a medium with anomalous dispersion of group velocity for various values of the saturation parameter  $\beta$  [ $\beta = 0$  (upper); 0.1; 0.2; 0.3; 0.5 (lower)].

### B. Ionization

In the framework of initial Eq. (6), the low-frequency (plasma) dispersion is determined by a parameter  $a$ . For the case of a gas breakdown, it is convenient to use the degree of plasma ionization as the parameter  $a$ . To describe the plasma formation dynamics, we will use the following equation from [19]

$$\frac{\partial a}{\partial \tau} = |u|^{2n}(a_0 - a). \quad (52)$$

Here, we assume the multiphoton ionization mechanism.

The dynamics of the self-action of initial wave fields having the form of Eq. (30) was modeled numerically basing on Eq. (6) in a medium with nonstationary nonlinear low-frequency dispersion described by Eq. (52). The parameter  $b$  was supposed to be equal to zero. It was assumed that the medium was not ionized in the absence of the field:  $a(\tau \rightarrow -\infty) = 0$ .

The results of numerical modeling demonstrate the following. For the field amplitude of order of the ionization threshold ( $u \sim 1$ ) the ionization influence is sufficient only at time intervals much larger than unity as it follows from Eq. (52). For sufficiently short pulse durations, the medium ionization, due to its inertia, does not have enough time to mani-

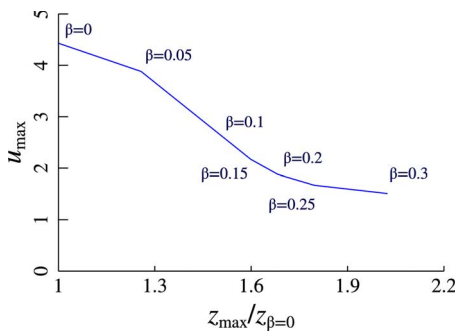


FIG. 11. (Color online) Dependence of the maximum field amplitude and self-focusing length on the nonlinearity saturation parameter  $\beta$ . Here,  $z_{max}$  is the length, along which the minimum size of the pulse is achieved,  $z^*$  is the self-focusing length for saturation-free case.

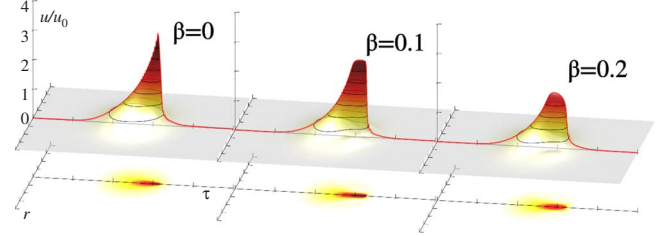


FIG. 12. (Color online) Distribution of the wave field with account for the nonlinearity saturation influence.

fest itself along the wave-breaking length [see Fig. 13(a) at  $\tau_0 = 3$ ] and, hence the self-action dynamics develops as if it were a dispersion-free medium (see Sec. IV).

As the pulse duration increases, the refraction in the produced plasma leads to widening of the wave packet (in the transverse direction) in the rear part of the pulse and to formation of flattening of the wave profile [see Figs. 13(a) and 13(b)], which is characteristic for the ionization nonlinearity. As the pulse duration (or the propagation path) increases further, the amplitude of the field on the axis drops down to the value being less than one on the periphery, and the wave packet becomes hollow for the most part (see Fig. 13). Competition of the Kerr (focusing) and ionization (defocusing) nonlinearities leads to a decrease in the maximum intensity of the field, and, therefore, to an increase in the wave-breaking length of the longitudinal wave profile.

Owing to the self-channeling regime, in this case, the nonlinear dispersion also leads to a wave-breaking of the longitudinal profile and formation of a shock wave. Thus, formation of rather sharp transitional areas takes place in the longitudinal direction in a wide range of pulse duration variations, which leads, consequently, to formation of power “tails” in the wave-field spectrum. Calculations show that the spectrum behavior is determined by the same power index, as in the case of self-action in a medium with anomalous dispersion (see Fig. 14).

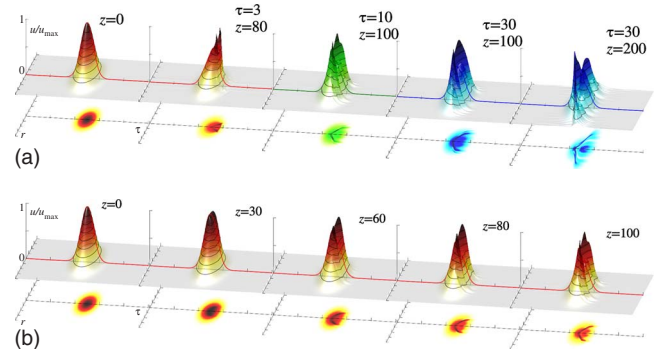


FIG. 13. (Color online) Results of numerical simulation of 3d pulse  $u(z, \tau, r)$  self-action taking into account media ionization: (a) for different initial pulse duration  $\tau_0 = 3, \tau_0 = 10, \tau_0 = 30$ ; (b) dynamics of the circularly polarized field with initial duration  $\tau_0 = 10$ . Media parameters are  $a_0 = 1, b = 0$ . Distribution of the circularly polarized field at the nonlinear-medium boundary  $u = e^{i\tau} \exp(-r_{\perp}^2/200 - \tau^2/\tau_0^2)$ .

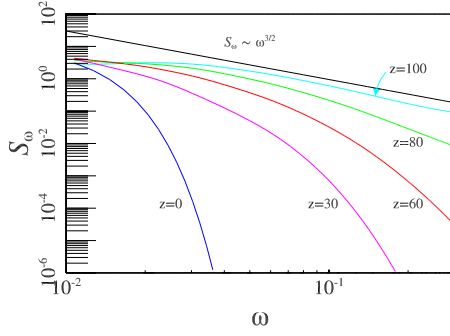


FIG. 14. (Color online) Short-wave part of the spectral power  $\int S^2(\omega > 1, r) r dr$  for  $z=0; 30; 60; 80; 100$  at  $a_0=1, b=0, \tau_0=10$ .

## VII. CONCLUSION

In this paper, we have developed an approach to studying the self-action of the wide-band pulses in a medium with inertia-free Kerr-type nonlinearity. We use the Eq. (6) first derived in [9]. At this, we pay special attention in our paper to the substantiation of its applicability in general media including regions of anomalous and normal dispersion of group velocity. This seems to be especially important when a noticeable widening of the spectrum takes place during the pulse propagation.

We have studied long-time evolution of three-dimensional wave packets and found a new class of equation solutions in media without dispersion and with anomalous dispersion. This is a new type of singularity when gradient catastrophe (wave breaking) develops while the field grows infinitely (“collapse”). The sufficient condition for the wave-field collapse is found [Eq. (13)]. At this, gradient catastrophe leads to formation of power-law tails in the pulse spectrum which is confirmed by numerical simulation (see Fig. 4). We derive the relation between the wave breaking and the collapse lengths and confirm it numerically (see Fig. 3). We obtain the critical power dependence on the pulse duration which again is confirmed numerically. Finally, taking into account the nonlinearity saturation and the ionization we found that gradient catastrophe still present even in these cases.

In this paper, we review self-action scenarios in general media (with anomalous and with normal dispersion) and pay special attention to the point of zero dispersion. The special class of initial pulse profiles is constructed for which the integral dispersion influence is compensated. Such pulses are collapsing when their duration is slightly enlarged. However the pulse spectrum modification is the most distinctive feature of a few-cycle pulse self-action in the vicinity of zero-dispersion point. Pulse spectrum becomes much wider (up to two octaves) and splits into two parts near the zero-

dispersion point  $\varpi \approx \omega_{bnd}$ . Such a strong modification of the spectrum of a laser pulse leads to formation of a spatiotemporal field distribution shaped as a corrugated surface (see Fig. 7).

## ACKNOWLEDGMENTS

This work was supported in part by the Russian Foundation for Basic Research (Projects No. 07-02-00596, No. 07-02-01239, No. 08-02-01260, and No. 08-02-00541). S.S. gratefully acknowledge the support by Dynasty Foundation and Russian Science Support Foundation.

## APPENDIX A: DISPERSION RELATION

Here we place the derivation procedure for the dielectric permittivity (8) based on general properties of dispersive media. Let us use Kramers-Kronig relation (see for example [12,14]),

$$\varepsilon_r(\omega) = 1 + \frac{2}{\pi} \int_0^{+\infty} \frac{x \varepsilon_i(x) dx}{x^2 - \omega^2}, \quad (\text{A1})$$

where  $\varepsilon_r$  and  $\varepsilon_i$  are the real and imaginary parts of the dielectric permittivity  $\varepsilon(\omega)$ . We will apply Eq. (A1) to weakly absorbing media (in the specified frequency range), i.e., we will assume that the imaginary part of the dielectric permittivity is negligible for this frequency range. Assume that the region of weak absorption spreads from  $\omega_1$  to  $\omega_2$  (where  $\omega_1 \ll \omega_2$ ) in some wide frequency range and consider such frequencies  $\omega$  that  $\omega_1 \ll \omega \ll \omega_2$ . The integration domain in Eq. (A1) is subdivided into three parts. In the first part, one can neglect  $x$  in the denominator of the integrand in comparison with  $\omega$ , whereas in the third part, the denominator can be expanded in a small parameter series  $\omega^2 \ll x^2$ ,

$$\begin{aligned} \varepsilon_r(\omega) = 1 + \frac{2}{\pi} & \left\{ \int_0^{\omega_1} \frac{x \varepsilon_i(x) dx}{x^2 - \omega^2} + \int_{\omega_1}^{\omega_2} \frac{x \varepsilon_i(x) dx}{x^2 - \omega^2} \right. \\ & \left. + \int_{\omega_2}^{+\infty} \frac{x \varepsilon_i(x) dx}{x^2 - \omega^2} \right\} \approx 1 + \frac{2}{\pi} \left\{ - \int_0^{\omega_1} \frac{x \varepsilon_i(x) dx}{\omega^2} \right. \\ & \left. + \int_{\omega_2}^{+\infty} \frac{\varepsilon_i(x) dx}{x \left( 1 - \frac{\omega^2}{x^2} \right)} \right\} \approx \hat{\varepsilon}_o + \hat{b} \omega^2 - \frac{\hat{a}}{\omega^2}, \quad (\text{A2}) \end{aligned}$$

where  $\hat{\varepsilon}_o = 1 + \frac{2}{\pi} \int_{\omega_2}^{+\infty} \frac{\varepsilon_i(x) dx}{x}$  is the static dielectric permittivity,  $\hat{a} = \frac{2}{\pi} \int_0^{\omega_1} x \varepsilon_i(x) dx$ , and  $\hat{b} = \frac{2}{\pi} \int_{\omega_2}^{+\infty} \frac{\varepsilon_i(x) dx}{x^3}$ . As is obvious, Eqs. (8) and (A2) have the same structure.

- [1] N. A. Zharova, A. G. Litvak, and V. A. Mironov, JETP Lett. **78**, 619 (2003); Sov. Phys. JETP **103**, 15 (2006).  
 [2] V. P. Kandidov, I. S. Golubtsov, and O. G. Kosareva, Quantum Electron. **34**, 348 (2004); L. Berge, S. Scupin, F. Lederer *et*

*al.*, Phys. Rev. Lett. **92**, 225002 (2004).

- [3] N. A. Zharova, A. G. Litvak, and V. A. Mironov, Radiophys. Quantum Electron. **46**, 297 (2003).  
 [4] Th. Brabec and F. Krausz, Rev. Mod. Phys. **72**, 545 (2000).

- [5] J. Ranka and A. Gaeta, *Opt. Lett.* **23**, 534 (1998); A. L. Gaeta, *Phys. Rev. Lett.* **84**, 3582 (2000); F. Bragheri, D. Faccio, A. Couairon, A. Matijosius, G. Tamosauskas, A. Varanavicius, V. Degiorgio, A. Piskarskas, and P. Di Trapani, *Phys. Rev. A* **76**, 025801 (2007).
- [6] L. Berge and S. Skupin, *Phys. Rev. E* **71**, 065601(R) (2005).
- [7] A. L. Gaeta, in *Self-focusing: Past and Present*, edited by R. W. Boyd, S. G. Lukishova, Y. R. Shen, Topics in Applied Physics Vol. 114, (Springer, New York, 2009) Chap. 16.
- [8] S. A. Akhmanov, B. A. Vislouxh, and A. S. Chirkin, *Optics of Femtosecond Laser Pulses* (AIP, New York, 1992); N. N. Akhmediev and A. Ankiewicz, *Solitons Nonlinear Pulses and Beams* (Chapman and Hall, London, 1997); Y. S. Kivshar and G. P. Agrawal, *Optical Solitons. From Fiber to Photonic Crystals* (Academic Press, New York, 2003).
- [9] A. A. Balakin, A. G. Litvak, V. A. Mironov, and S. A. Skobelev, *Sov. Phys. JETP* **104**, 363 (2007).
- [10] S. A. Kozlov and S. V. Sazonov, *Sov. Phys. JETP* **84**, 221 (1997); A. N. Berkovsky, S. A. Kozlov, and Y. A. Shpolyanskiy, *Phys. Rev. A* **72**, 043821 (2005).
- [11] A. G. Litvak, V. A. Mironov, and S. A. Skobelev, *JETP Lett.* **82**, 105 (2005).
- [12] S. A. Skobelev, D. V. Kartashov, and A. V. Kim, *Phys. Rev. Lett.* **99**, 203902 (2007).
- [13] V. E. Semenov, *Sov. Phys. JETP* **102**, 34 (2006).
- [14] L. D. Landau and E. M. Lifshitz, *Course of Theoretical Physics*, 2nd ed. (Nauka, Moscow, 1982; Pergamon, Oxford, 1984), Vol. 8: Electrodynamics of Continuous Media.
- [15] D. V. Kartashov, A. V. Kim, and S. A. Skobelev, *JETP Lett.* **78**, 276 (2003); S. A. Skobelev and A. V. Kim, *ibid.* **80**, 623 (2004).
- [16] L. D. Landau and E. M. Lifshitz, *Course of Theoretical Physics*, 3rd ed. (Nauka, Moscow, 1986; Pergamon, New York, 1987), Vol. 6: Fluid Mechanics.
- [17] S. N. Vlasov and V. I. Talanov, *Wave Self-Focusing* (Institute of Applied Physics of the Russian Academy of Science, Nizhny Novgorod, 1997).
- [18] N. A. Zharova, A. G. Litvak, T. A. Petrova, A. M. Sergeev, and A. D. Yunakovskii, *JETP Lett.* **44**, 13 (1986).
- [19] L. Berge, *Phys. Rep.* **303**, 259 (1998); A. Couairon and A. Mysyrowicz, *ibid.* **441**, 47 (2007).
- [20] A. A. Balakin, A. G. Litvak, V. A. Mironov, and S. A. Skobelev, *Phys. Rev. A* **78**, 061803(R) (2008).